Numerical Study of Water Depth Effect on Sway Velocity and Rudder Derivatives of a Container Ship in Manoeuvring

Akhil Balagopalan and P. Krishnankutty

Abstract Correct prediction of the hydrodynamic derivatives is essential for the accurate determination of ships manoeuvring performance. Numerical and experimental methods are widely used for the determination of these derivatives. Even though experimental methods are more reliable, these facilities are rare and often prohibitively expensive. More viable option, primarily during the early stages of the ship design, is to determine these derivatives numerically. And also most of the ship manoeuvring studies and regulations are on deep water conditions, whereas the ship manoeuvring performance is much worse in shallow waters, and its controllability is difficult. An attempt is made in this paper to study the shallow water effects on the sway velocity-dependent derivatives and rudder derivatives numerically. KRISO container ship (KCS), a benchmark example used by different research groups, is taken for the present study. Straight line or static drift tests are performed in a numerical environment at different drift and different rudder angles using a commercial CFD package. These tests are conducted in both deep and shallow water conditions. Effects of water depth on the sway velocity-dependent hydrodynamic derivatives and rudder derivatives are evaluated, and the results are presented and analysed.

Keywords KCS · Manoeuvring · Straight line test · Hydrodynamic derivative CFD

1 Introduction

Manoeuvring quality assessment for seagoing vessels is essential for the navigational safety purpose. International Maritime Organization (IMO) has prescribed guidelines for the seagoing vessels to ensure its navigational safety as well as operational effi-

A. Balagopalan (✉) · P. Krishnankutty
Department of Ocean Engineering, IIT Madras, Chennai, India
e-mail: bgakhil@gmail.com

P. Krishnankutty
e-mail: pkrishnankutty@iitm.ac.in

K. Murali et al. (eds.), *Proceedings of the Fourth International Conference in Ocean Engineering (ICOE2018)*, Lecture Notes in Civil Engineering 22,
https://doi.org/10.1007/978-981-13-3119-0_16

ciency during its voyage. Manoeuvring quality of a ship primarily depends on the hull geometry and is to be essentially determined in its initial stage of design. The surface ship manoeuvrability is governed by the equations of motions in surge, sway and yaw motions which are relevant motions in the horizontal plane. The directional stability and control characteristics of a ship are generally understood by solving these manoeuvring equations of motion for which the knowledge of hydrodynamic derivatives are important. Accurate prediction of hydrodynamic derivatives determines the quality of prediction of the manoeuvring characteristic of vessel such as turning ability and course keeping ability rudder effectiveness. Empirical relations given by researchers [1, 2] give a rough estimate of the hydrodynamic derivatives but fail to predict higher order and coupled non-linear derivatives. Numerical and experimental methods are widely used for the estimation of hydrodynamic derivatives. Even though experimental methods are more reliable, these facilities are rare and often prohibitively expensive. More viable option, primarily during the early stages of the ship design, is to determine these derivatives numerically.

In shallow water, the flow around the vessel modifies drastically and thus the hydrodynamic derivatives also. Ships operating in these regions become sluggish and behave poorly to the action of control surfaces. Hence, the correct estimation of hydrodynamic derivatives in shallow water is inevitable to predict the vessels manoeuvring behaviour when it is operating in water depth-restricted regions such as ports, harbours, inland waterways. Experimental facilities for shallow water manoeuvring studies are very rare all over the world. With the advancement of computational techniques, the application of computational fluid dynamic (CFD) is emerging as a powerful tool for the prediction of ship manoeuvring performance even for different water depth conditions. The manoeuvring performance results obtained from CFD are promising and are reliable when compared to the actual ships manoeuvring performance [3–5]. This paper presents the influence of water depth on the velocity derivatives Y_v, N_v, Y_{vvv}, N_{vvv} and rudder derivatives Y_δ, N_δ, $Y_{\delta\delta\delta}$ and $N_{\delta\delta\delta}$. Stationary straight line tests with different drift angles and rudder angles were conducted using commercial CFD software STAR-CCM+. Numerical simulations were conducted for both deep water and shallow water conditions. Shallow water condition as $H/T = 1.5$ is taken for the current study.

2 Nomenclature

B	Beam (m)
CB	Block coefficient
CM	Midship area coefficient
D	Depth (m)
H	Water height (m)
L_{oa}	Length overall (m)
L_{pp}	Length between perpendiculars (m)
L_{wl}	Load water line (m)

N_v Hydrodynamic linear coupled derivative of yaw moment with respect to sway velocity
N_{vvv} Hydrodynamic third-order coupled derivative of yaw moment with respect to sway velocity
N_δ Hydrodynamic linear coupled derivative of yaw moment with respect to rudder deflection
$N_{\delta\delta\delta}$ Hydrodynamic third-order coupled derivative of yaw moment with respect to rudder deflection
T Draft (m)
Y_v Hydrodynamic linear coupled derivative of sway force with respect to sway velocity
Y_{vvv} Hydrodynamic third-order coupled derivative of sway force with respect to sway velocity
Y_δ Hydrodynamic linear coupled derivative of sway force with respect to rudder deflection
$Y_{\delta\delta\delta}$ Hydrodynamic third-order coupled derivative of sway force with respect to rudder deflection
V Forward velocity of the ship (m/s)
v Sway velocity (m/s)
β Drift angle (°)
δ Rudder angle (°)

3 Straight Line Test

Sway velocity and rudder derivatives are found out by simulating the straight line test in CFD environment. Straight line tests are conducted for different drift angles ($\beta = 3, 6, 9, 12, 15, 18$) to estimate the sway velocity derivatives Y_v, Y_{vvv}, N_v and N_{vvv}, (Fig. 1). Rudder derivatives Y_δ, $Y_{\delta\delta\delta}$, N_δ and $N_{\delta\delta\delta}$ are estimated by giving different rudder angles ($\delta = 5, 10, 15, 20, 25, 30, 35$) to the vessel with zero drift angle (Fig. 2). Numerical simulations are carried out for both deep water ($H/T > 3$) and for shallow water ($H/T = 1.5$) conditions.

4 Hull Geometry

The KRISO container ship (KCS) model, a benchmark model being used by different research groups worldwide, has been chosen for the present study. The main particulars of the vessel and model details are shown in Table 1.

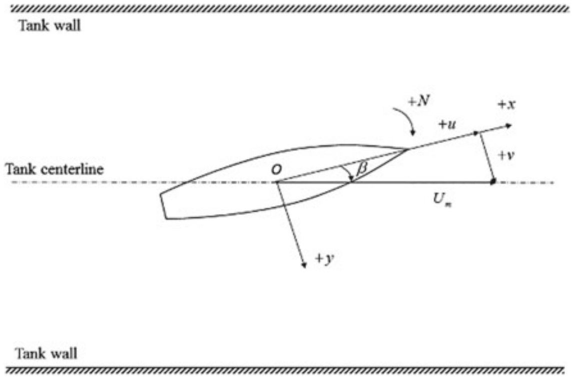

Fig. 1 Model with drift angle

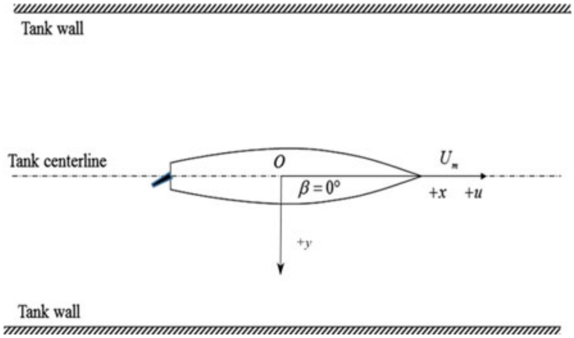

Fig. 2 Model with rudder deflection

Table 1 Particulars of the container ship

Main particulars	Full scale	Model (1:75.5)
L_{pp} (m)	230.0	3.0464
L_{wl} (m)	232.5	3.0791
B_{wl} (m)	32.2	0.4265
D (m)	19.0	0.2517
T (m)	10.8	0.1430
Displacement (m^3)	52030	0.1209
S w/o rudder (m^2)	9530	1.6719
CB	0.651	0.651
CM	0.985	0.98

5 Numerical Study

Commercial CFD package STAR-CCM+ is used for the present study. Solver settings for both deep and shallow water conditions are given in Table 2.

Table 2 Computational parameters

Solver	3-D segregated implicit unsteady
Temporal discretization	Second order
Turbulence model	k-epsilon
Wall treatment	All wall y+
Free surface modelling	VOF method
Time step	0.01
Maximum physical time	50 s

Table 3 Domain dimensions

Direction	Deep water (L_{oa})	Shallow water (L_{oa})
Forward	1.5	1.5
Aft	2.5	2.5
Side	2	2
Deck to top	1.5	1.5
Keel-bottom	1.5	0.022

Table 4 Boundary conditions

Inlet	Velocity inlet
Outlet	Pressure outlet
Top	Velocity inlet
Side	Wall with slip
Bottom	Wall with no slip
Hull	No slip wall

5.1 Computational Domain

Fluid domain (Table 3) is selected based on the ITTC Standards [6]. Two different computational domains are created based on deep water ($H/T = 25$) (Fig. 3) and shallow water ($H/T = 1.5$) (Fig. 4) conditions. The boundary conditions (Table 4) are applied to the computational domain for the analysis. Wave damping option is enabled at the side wall boundaries to avoid wave reflections.

5.2 Mesh Generation

Unstructured trimmed hexahedral mesh is generated with near wall prismatic layers using CFD tool (Figs. 5 and 6). Three separate volumetric blocks at bow, stern and free surface are created with refined mesh density. Separate meshes are generated for

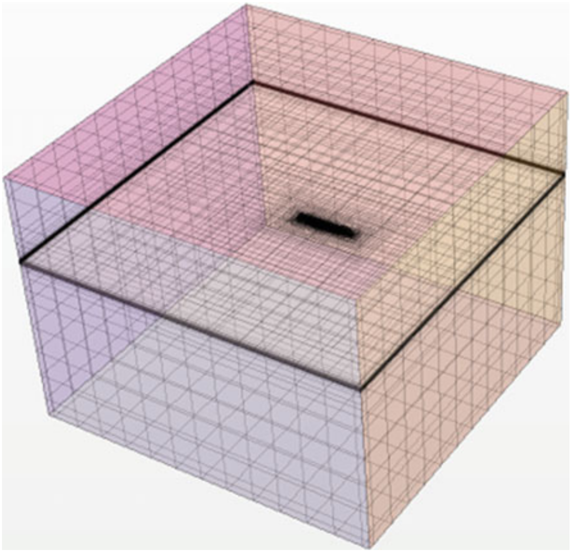

Fig. 3 Deep water domain

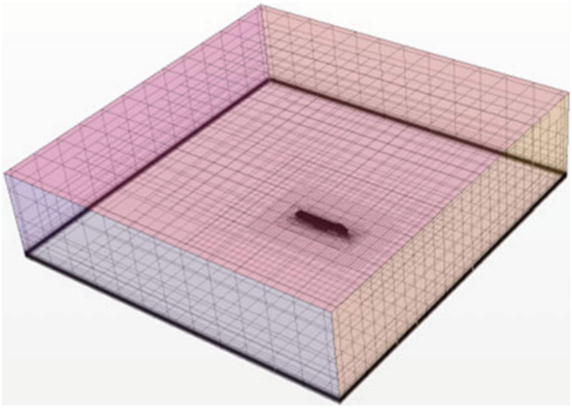

Fig. 4 Shallow water domain

different drift angles and for different rudder angles for each simulation trials. Mesh generated for 9° drift angle (Fig. 7) and 20° rudder angle (Fig. 8) is given below.

6 Grid Independence Study

Grid independence study is performed to ensure that the results are unaffected by the base size/number of cells. Four different grid sizes are selected to analyse the grid dependency. Inflow velocity of 1.1 m/s is given to the ship model, and the total resistance is estimated. It is observed that there is not much variation exists between

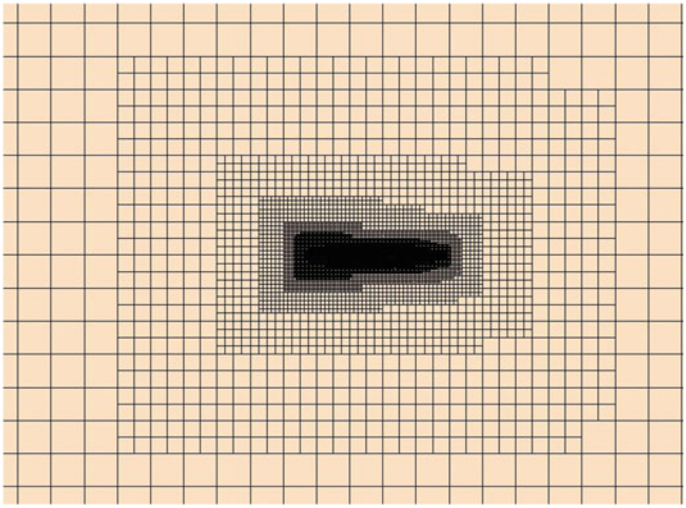

Fig. 5 Generated mesh

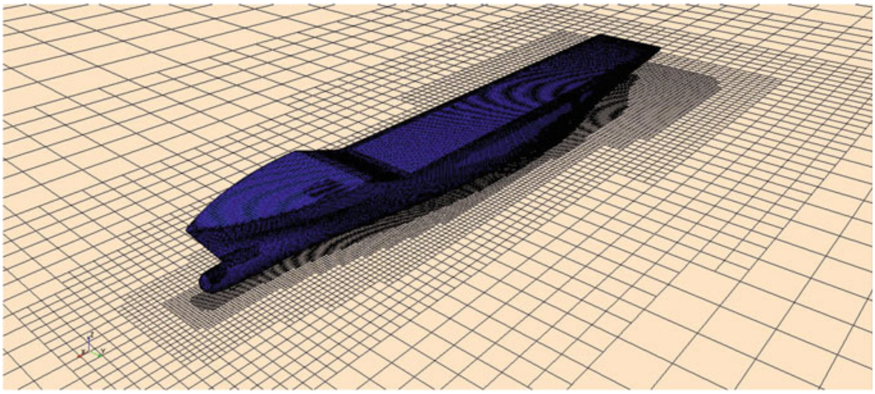

Fig. 6 Mesh configuration around the vessel

the base sizes 0.1 and 0.085. Hence, the base size of 0.1 m with 1.7 million cells is selected. Grid independence test results are given in Table 5.

7 Grid Validation with CFD and Experimental Results

Numerical CFD resistance test for KCS model is conducted for different speeds with the same generated mesh condition, 0.1 m of base size and 1.7 million cells .

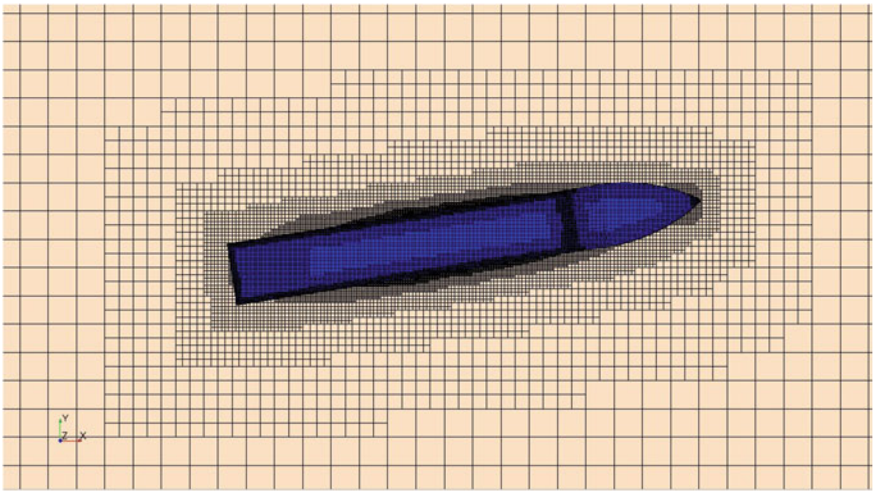

Fig. 7 Ship at 9° drift angle

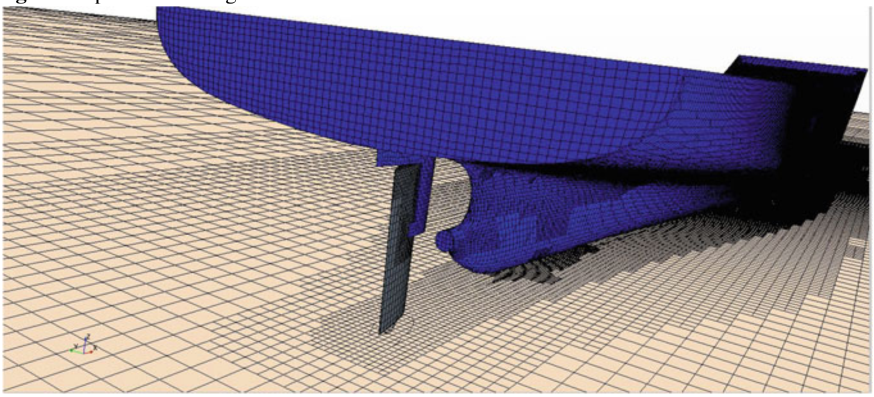

Fig. 8 Ship at 20° rudder angle

Experimental resistance test (Fig. 9) is conducted at IIT Madras towing tank facility where the model is towed at different speeds, and the total resistance is measured at

Table 5 Grid independence study results

No.	Base size (m)	Number of cells (millions)	Resistance (N)
1	0.15	1.1	4.78
2	0.1	1.7	4.541
3	0.085	2.2	4.533
4	0.07	2.9	4.17

Fig. 9 KCS resistance test arrangement

Table 6 CFD and experimental resistance test results

Model speed (m/s)	Resistance (N)	
	CFD	Experimental
0.7	2.182	–
0.77	2.461	2.71
0.829	2.801	2.67
0.888	3.17	2.95
0.947	3.56	3.36
1.066	4.24	4.27
1.1	4.54	4.44
1.125	4.722	4.66
1.184	5.129	5.07
1.243	5.608	5.56
1.302	6.195	6.01
1.362	6.865	6.66
1.421	7.696	7.51
1.48	9.032	8.81
1.539	10.605	10.65

its design displacement. CFD and experimental resistance test results are given in Table 6, and the same are compared in Fig. 10. The values closely match, and hence, the same grid is used for numerical analysis.

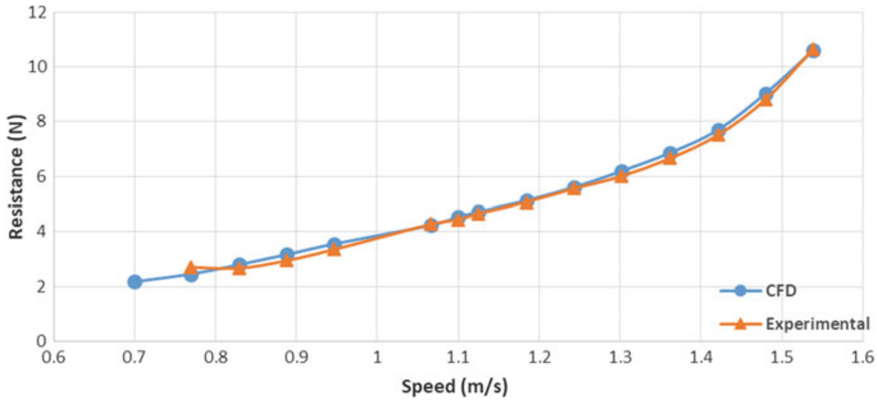

Fig. 10 CFD and experimental result comparison

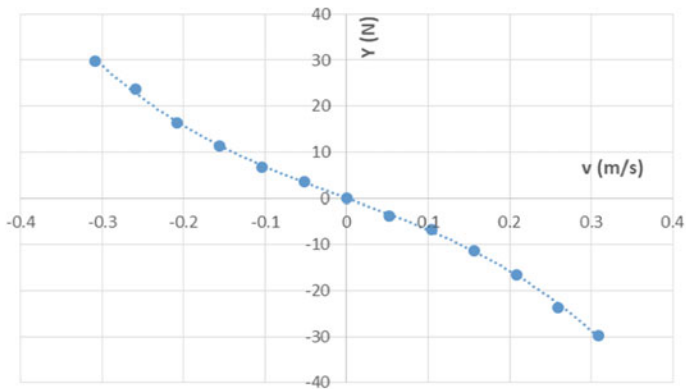

Fig. 11 Plot of sway force against sway velocity

8 Numerical Tests, Results and Discussions

Straight line tests are conducted for both deep water and shallow water conditions.

8.1 Deep Water Condition

8.1.1 Sway Velocity Derivatives

Sway force and yaw moment acting on the vessel at its centre of gravity are estimated for different drift angles. These forces are plotted against the sway velocity v (Figs. 11 and 12). The sway velocity is given by

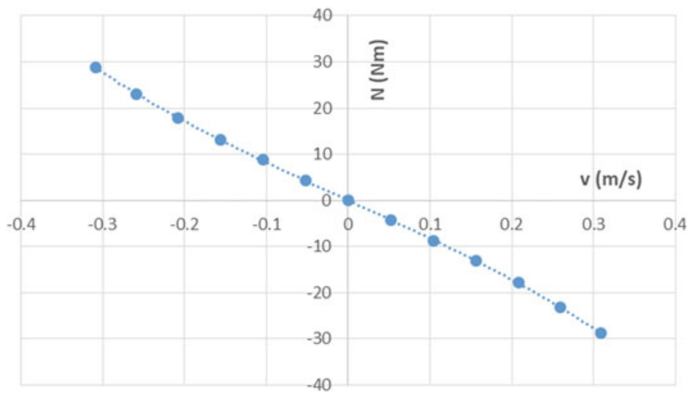

Fig. 12 Plot of yaw moment against sway velocity

$$v = -V \sin \beta \tag{1}$$

The hydrodynamic derivatives are calculated by taking the slope of the curve at $v = 0$. Tests are conducted only to port side drift angle of the vessel, and values are mirrored by considering ship symmetry about its central longitudinal vertical plane. Y_v, N_v, Y_{vvv}, N_{vvv} are non-dimensionalised by using the following relations (Table 7).

$$Y'_v = \frac{Y_v}{0.5\rho \, \mathrm{Lwl}^2 V} \tag{2}$$

$$N'_v = \frac{N_v}{0.5\, \rho \, \mathrm{Lwl}^3 V} \tag{3}$$

$$Y'_{vvv} = \frac{Y_{vvv}}{(0.5\, \rho \, \mathrm{Lwl}^2)/V} \tag{4}$$

$$N'_{vvv} = \frac{N_{vvv}}{(0.5\, \rho \, \mathrm{Lwl}^3)/V} \tag{5}$$

Table 7 Straight line test results

Drift angle (°)	Sway velocity v (m/s)	Y force (N)	N moment (N m)
0	0.000	0	0
3	−0.052	3.673	4.297
6	−0.105	6.721	8.869
9	−0.156	11.285	13.073
12	−0.208	16.466	17.776
15	−0.259	23.621	23.089
18	−0.309	29.802	28.769

Third-order cubical curves are fitted on the above plots. Curves fitted with third-order polynomial in non-dimensional format are given below.

$$Y' = -0.0729712\, v'^3 - 0.013726\, v' + 7 \times 10^{-13} \tag{6}$$

$$N' = -0.0086672\, v'^3 - 0.005556\, v' - 8 \times 10^{-13} \tag{7}$$

Hydrodynamic derivatives are obtained by differentiating the above equation with respect to sway velocity, v at $v = 0$ and equating the terms with that of Taylor series representation of force and moment. The order of differentiation depends on the order of derivatives to be estimated. Equating the likely terms with Taylor series will give the following relation for the hydrodynamic derivatives.

$$Y'_v = \left[\frac{\partial Y'}{\partial v'}\right] \quad \text{at } v = 0 \tag{8}$$

$$Y'_{vvv} = \frac{1}{3!}\left[\frac{\partial^3 Y'}{\partial v^3}\right] \quad \text{at } v = 0 \tag{9}$$

$$N'_v = \left[\frac{\partial N'}{\partial v'}\right] \quad \text{at } v = 0 \tag{10}$$

$$N'_{vvv} = \frac{1}{3!}\left[\frac{\partial^3 N'}{\partial v'^3}\right] \quad \text{at } v = 0 \tag{11}$$

The non-dimensional hydrodynamic derivatives estimated are

$$Y'_v = -0.013726$$
$$Y'_{vvv} = -0.0729712$$
$$N'_v = -0.005556$$
$$N'_{vvv} = -0.0086672$$

8.1.2 Rudder Derivatives

Sway force and moment acting at the centre of gravity of the vessel for different rudder angles are estimated from the CFD analysis (Table 8). These are plotted against rudder angle (Figs. 13 and 14). The data is fitted with a third-order cubic polynomial curve and is represented in non-dimensional format as below.

$$Y' = -0.00121289\, \delta'^3 + 0.00112811\, \delta' - 5 \times 10^{-14} \tag{12}$$

$$N' = +0.00048225\, \delta'^3 - 0.000466305\, \delta' + 2 \times 10^{-12} \tag{13}$$

Rudder derivatives are non-dimensionalised by using the following relations.

$$Y'_\delta = \frac{Y_\delta}{0.5\rho\, \mathrm{Lwl}^2 V} \tag{14}$$

Table 8 Rudder forces and moments

Rudder angle δ (°)	Y force (N)	N moment (N m)
0	0	0
5	0.536	−0.63
10	0.999	−1.274
15	1.339	−1.726
20	1.528	−1.97
25	1.799	−2.29
30	1.968	−2.562
35	1.98	−2.577

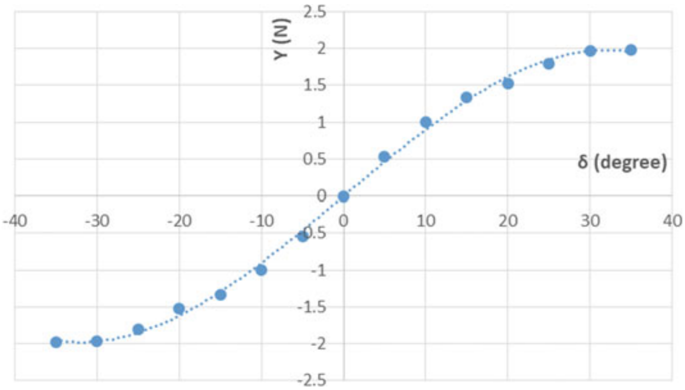

Fig. 13 Sway force plotted against rudder angle

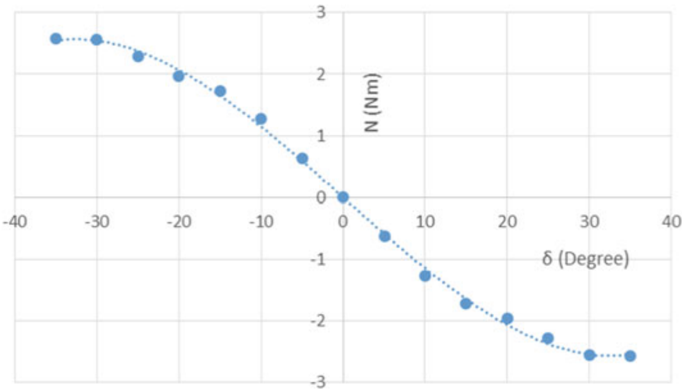

Fig. 14 Yaw moment plotted against rudder angle

$$N'_\delta = \frac{N_\delta}{0.5\rho \,\mathrm{Lwl}^3 V} \tag{15}$$

$$Y'_{\delta\delta\delta} = \frac{Y_{\delta\delta\delta}}{(0.5\rho\,\mathrm{Lwl}^2)/V} \tag{16}$$

$$N'_{\delta\delta\delta} = \frac{N_{\delta\delta\delta}}{(0.5\rho\,\mathrm{Lwl}^3)/V} \tag{17}$$

Hydrodynamic rudder derivatives are obtained by differentiating the non-dimensional Eqs. 12 and 13 with respect to rudder angle, δ at $\delta = 0$ and equating the terms with that of Taylor series representation of force and moment. Order of differentiation depends on the order of requirement of derivatives. Expression for rudder derivatives is listed below.

$$Y'_{\delta} = \left[\frac{\partial Y'}{\partial \delta'}\right] \quad \text{at } \delta = 0 \tag{18}$$

$$Y'_{\delta\delta\delta} = \frac{1}{3!}\left[\frac{\partial^3 Y'}{\partial \delta'^3}\right] \quad \text{at } \delta = 0 \tag{19}$$

$$N'_{\delta} = \left[\frac{\partial N'}{\partial \delta'}\right] \quad \text{at } \delta = 0 \tag{20}$$

$$N'_{\delta\delta\delta} = \frac{1}{3!}\left[\frac{\partial^3 N'}{\partial \delta'^3}\right] \quad \text{at } \delta = 0 \tag{21}$$

Estimated non-dimensional rudder derivatives are given below.

$$\begin{aligned} Y'_{\delta} &= 0.00112811 \\ Y'_{\delta\delta\delta} &= -0.00121289 \\ N'_{\delta} &= -0.000466305 \\ N'_{\delta\delta\delta} &= +0.000482255 \end{aligned}$$

8.2 Shallow Water Condition

8.2.1 Sway Velocity Derivatives

Numerical simulations are repeated for shallow water condition with $H/T = 1.5$. Sway forces and yaw moments are estimated for different drift angles (Table 9). These values are plotted against sway velocity (Figs. 15 and 16). Third-order polynomial is fitted on the plot. This gives the cubic polynomial expression for sway force and yaw moment in non-dimensional format as

$$Y' = -0.483601\, v'^3 - 0.02919\, v' + 4 \times 10^{-12} \tag{22}$$

$$N' = -0.055701\, v'^3 - 0.012297\, v' - 3 \times 10^{-13} \tag{23}$$

Table 9 Straight line test results

Drift angle (°)	Sway velocity v (m/s)	Y force (N)	N moment (Nm)
0	0.000	0	0
3	−0.052	7.997	9.43
6	−0.105	15.748	19.239
9	−0.156	30.759	30.554
12	−0.208	47.585	45.031
15	−0.259	78.351	60.777
18	−0.309	108.798	78.832

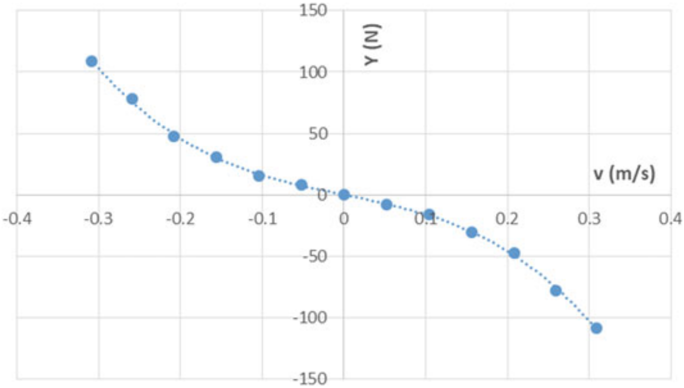

Fig. 15 Plot of sway force against sway velocity

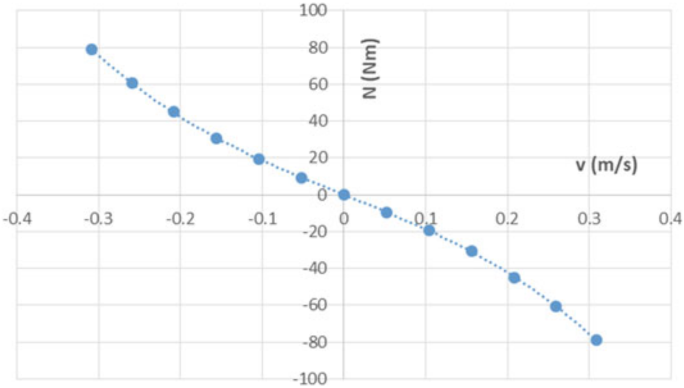

Fig. 16 Plot of yaw moment against sway velocity

Hydrodynamic derivatives are estimated by using Eqs. 8, 9, 10 and 11. Estimated derivatives are given below.

$$Y'_v = -0.02919$$

Table 10 Rudder forces and moments

Rudder angle δ (°)	Y force (N)	N moment (N m)
0	0	0
5	0.365	−0.353
10	0.719	−0.681
15	0.999	−1.006
20	1.06	−1.153
25	1.273	−1.389
30	1.444	−1.631
35	1.499	−1.677

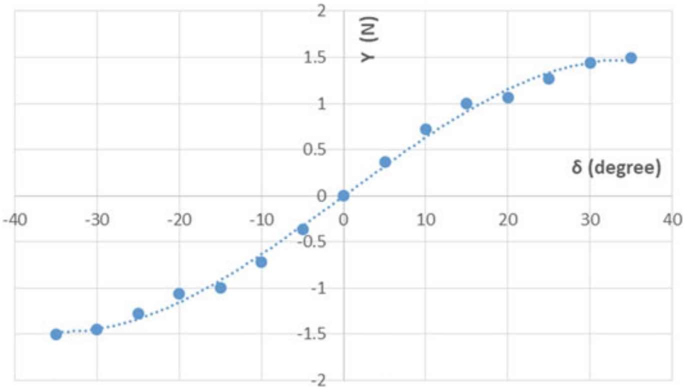

Fig. 17 Sway force plotted against rudder deflections

$$Y'_{vvv} = -0.483601$$
$$N'_{v} = -0.012297$$
$$N'_{vvv} = -0.055701$$

8.2.2 Rudder Derivatives

Rudder derivatives are estimated by measuring the sway force and yaw moment acting at the centre of gravity of the vessel in shallow water condition (Table 10). These values are plotted against rudder angle (Figs. 17 and 18). Third-order polynomial curve is fitted on the graph and is represented in non-dimensional format as below.

$$Y' = -0.000758721\,\delta'^3 + 0.00079154\,\delta' - 4 \times 10^{-14} \quad (24)$$
$$N' = 0.000199038\,\delta'^3 - 0.00026332\,\delta' - 2 \times 10^{-12} \quad (25)$$

The derivatives are estimated by taking the slope of the curve at $\delta = 0$ by using Eqs. 14, 15, 16 and 17. Rudder derivatives estimated are given below.

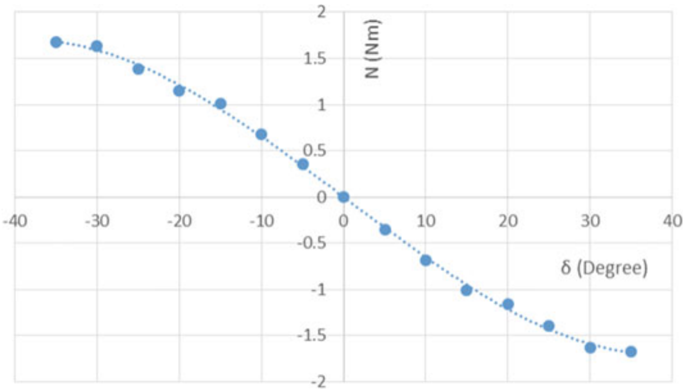

Fig. 18 Yaw moment plotted against rudder deflections

$$Y'_{\delta} = 0.00079154$$
$$Y_{\delta\delta\delta} = -0.000758721$$
$$N'_{\delta} = -0.00026332$$
$$N'_{\delta\delta\delta} = +0.000199038$$

9 Summary and Conclusion

In the present study, straight line tests are conducted with different drift angles and rudder angles for both deep water and shallow water conditions. Numerical analysis clearly indicates the influence of water depth on these hydrodynamic derivatives. Sway velocity derivatives Y'_v and N'_v in shallow water show a variation of -112.65 and -121.18%, respectively, compared to that in deep water condition. Third-order derivatives Y'_{vvv} and N'_{vvv} show drastic variation of -562.73 and -542.66% from deep water to shallow water condition. Shallow water effect has a negative influence on the rudder performance too, as expected due to the inferior flow conditions. Y'_{δ} and N'_{δ} in shallow water are 26.3 and 44.1% higher than that in deep water. $Y'_{\delta\delta\delta}$ and $N'_{\delta\delta\delta}$ also follow the same trend and varies 37.45 and 60.6%, respectively, when water depth changes from deep to shallow. The numerical study clearly shows the effects of water depth on the manoeuvring performance of the container ship. This study can be further extended by estimating the acceleration derivatives and by simulating the turning trajectory of the vessel.

References

1. Inoue S, Hirano M, Kijima K (1981) Hydrodynamic derivatives on ship maneuvering. Int Ship Building Prog 28(321):112–125
2. Kijima K, Nakari Y, Furukawa Y (2000) On prediction method for ship manoeuvrability. In: Proceedings of international workshop on ship manoeuvrability at Hamburg ship model basin, paper no. 7, Hamburg, Germany
3. Carrica PM, Ismail F, Hyman M, Bhushan S, Stern F (2013) Turn and zig-zag maneuvers of surface combatant using URANS approach with dynamic overset grids. J Mar Sci Technol 18:166–181
4. Cura-Hochbaum A (2011) On the numerical prediction of the ship's manoeuvring behaviour. Ship Sci Technol 5(9):27–39
5. Delefortrie G, Vantorre M (2007) Modeling the maneuvering behaviour of container carriers in shallow water. J Ship Res 51(4):287–296
6. ITTC recommended procedures (2011) Guidelines on use of RANS tools for ManeuverinPrediction. In: Proceedings of 26th ITTC